Atmos. Chem. Phys., 16, 7485–7496, 2016
www.atmos-chem-phys.net/16/7485/2016/
doi:10.5194/acp-16-7485-2016

Atmospheric Chemistry and Physics
Open Access
EGU

New particle formation in the fresh flue-gas plume from a coal-fired power plant: effect of flue-gas cleaning

Fanni Mylläri[1], Eija Asmi[2], Tatu Anttila[1], Erkka Saukko[1], Ville Vakkari[2], Liisa Pirjola[3], Risto Hillamo[2], Tuomas Laurila[2], Anna Häyrinen[4], Jani Rautiainen[4], Heikki Lihavainen[2], Ewan O'Connor[2], Ville Niemelä[5], Jorma Keskinen[1], Miikka Dal Maso[1], and Topi Rönkkö[1]

[1]Department of Physics, Tampere University of Technology, P.O. Box 692, 33101 Tampere, Finland
[2]Atmospheric Composition Research, Finnish Meteorological Institute, 00560, Helsinki, Finland
[3]Department of Technology, Metropolia University of Applied Sciences, 00180, Helsinki, Finland
[4]Helen Oy, 00090 Helen, Helsinki, Finland
[5]Dekati Ltd., Tykkitie 1, 36240 Kangasala, Finland

Correspondence to: Topi Rönkkö (topi.ronkko@tut.fi)

Received: 8 December 2015 – Published in Atmos. Chem. Phys. Discuss.: 5 February 2016
Revised: 24 May 2016 – Accepted: 30 May 2016 – Published: 15 June 2016

Abstract. Atmospheric emissions, including particle number and size distribution, from a 726 MW_{th} coal-fired power plant were studied experimentally from a power plant stack and flue-gas plume dispersing in the atmosphere. Experiments were conducted under two different flue-gas cleaning conditions. The results were utilized in a plume dispersion and dilution model taking into account particle formation precursor (H_2SO_4 resulted from the oxidation of emitted SO_2) and assessment related to nucleation rates. The experiments showed that the primary emissions of particles and SO_2 were effectively reduced by flue-gas desulfurization and fabric filters, especially the emissions of particles smaller than 200 nm in diameter. Primary pollutant concentrations reached background levels in 200–300 s. However, the atmospheric measurements indicated that new particles larger than 2.5 nm are formed in the flue-gas plume, even in the very early phases of atmospheric ageing. The effective number emission of nucleated particles were several orders of magnitude higher than the primary particle emission. Modelling studies indicate that regardless of continuing dilution of the flue gas, nucleation precursor (H_2SO_4 from SO_2 oxidation) concentrations remain relatively constant. In addition, results indicate that flue-gas nucleation is more efficient than predicted by atmospheric aerosol modelling. In particular, the observation of the new particle formation with rather low flue-gas SO_2 concentrations changes the current understanding of the air quality effects of coal combustion. The results can be used to evaluate optimal ways to achieve better air quality, particularly in polluted areas like India and China.

1 Introduction

On the global scale, nearly 40 % of annual production of electricity is covered by coal combustion (EU, 2014). In addition to CO_2 emissions, known to have climatic effects, coal combustion causes emissions of other harmful pollutants like NO_x, SO_2 and particulate matter, all decreasing the air quality and increasing health-related risks but also affecting climate directly and indirectly. For instance, SO_2 affects the climate indirectly because it tends to oxidize in atmosphere and form H_2SO_4, which affects particle formation. Coal-combustion-related air quality problems exist, especially in developing countries like China (Huang et al., 2014), where power production is not always equipped with efficient flue-gas cleaning systems. However, with proper combustion and flue-gas cleaning technologies the fine particle emissions of coal combustion can be decreased to a very low level and the emissions of gaseous pollutants other than CO_2 can also be decreased (Helble, 2000; Saarnio et al., 2014). Particle mass and number emission factors for the 300 MW coal-fired power plant with electrostatic precipitator (ESP) and flue-gas desulfurization unit (FGD) have been

reported by Frey et al. (2014): the emission for particle mass (PM_1) was 0.18 ± 0.06 mg MJ^{-1} and for fine particle number $2.3 \times 10^9 \pm 4.0 \times 10^9$ MJ^{-1}. However, it can be expected that particle emissions and characteristics such as particle size are highly dependent on technologies used in power production. Only a few studies have reported particle number size distributions and mean particle diameter for the coal combustion emissions. The mean particle diameters have been reported to be between 100 nm (Frey et al., 2014; Yi et al., 2008) and 1 µm (Yi et al., 2008; Lee et al., 2013). According to Saarnio et al. (2014), chemical composition of particles in the efficiently cleaned flue gas after the FGD is shifted towards desulfurization chemicals. Interestingly, sulfate particle emissions from coal combustion with proper cleaning technologies can restrain global warming due to a cooling effect of the particles (Frey et al., 2014; Charlson et al., 1992; Lelieveld and Heintzenberg, 1992).

Due to the emission limits of power plants, driven by the need for a healthier environment, emissions should be kept at minimum. This can be achieved by different technologies. Flue-gas NO_x emissions can be reduced in the power plant boiler by applying low-NO_x burners, whereas SO_2 emissions can be reduced by flue-gas desulfurization (FGD) (Srivastava and Jozewicz, 2001). Particle emissions can be reduced by electrostatic precipitators (ESP) and fabric filters (FF). Very low emission levels can be achieved by these techniques. For example, for particle emission, ESP typically removes 99 % (Helble, 2000) of fine particles. Further, Saarnio et al. (2014) showed that a desulfurization plant with fabric filters removes up to 97 % of fine particles. A combination of these techniques would then remove 99.97 % of fine particle emissions formed in combustion. However, particle emission as well as the effects of technologies can differ if the emissions are measured from the diluted flue gas in the atmosphere. In principle, particle number and even particle mass can increase in the atmosphere, for example, due to nucleation and condensation processes (Marris et al., 2012; Buonanno et al., 2012). However, there are very few observations of the processes in the diluting flue gas during the first few minutes after the stack.

Power plant plumes have been studied with aircraft by measuring long-distance crosswind profiles of gases and particles (Stevens et al., 2012; Brock et al., 2002; Lonsdale et al., 2012; Junkermann et al., 2011). Stevens et al. (2012) and Lonsdale et al. (2012) have compared these measurements to modelling results, which were based on emission inventory values. Modelling results indicated that secondary particle formation occurs in the plumes after emission from the stack and the measurement results show correlation with the model especially at distances of 10–20 km. Brock et al. (2002) argue that the secondary particle formation begins in a 2 h old plume. A study by Brock et al. (2002) has focused on 0 to 13 h old power plant plumes. However, Brock et al. (2002) do not report particle number concentrations for fresh flue gas. Crosswind profiles shown in the study of Stevens et al. (2012) were at distances from 5 km to a little over 50 km, and these results were also used in Lonsdale et al. (2012). On the contrary, Junkermann et al. (2011) followed the plume centre line based on the SO_2 concentrations and also made a few crosswind profiles of the studied plume.

The aim of this study was to characterize how the atmospheric emissions from a 726 MW coal-fired power plant depend on flue-gas cleaning, i.e. desulfurization plant and fabric filters (later referred to as "FGD + FF off" and "FGD + FF on"). In addition to the stack measurements for pollutants, the study aimed to show how the flue-gas cleaning affects real atmospheric concentrations of emitted CO_2, SO_2 and particles. The study included experiments conducted in the stack of the power plant, measurements conducted with a helicopter equipped with instruments for CO_2, SO_2 and particles and flue-gas plume dispersion and aerosol process modelling.

2 Experimentation

The studied power plant is a base-load station located near Helsinki city centre, Finland. The power plant consists of two 363 MW_{th} coal-fired boilers. The energy is produced by coal combustion in 12 low-NO_x technology burners (Tampella/Babcock-Hitachi HTNR low-NO_x), situated at the front wall of the boiler. The properties of coal used in this study are listed in Table S1 in the Supplement. Combustion releases flue gases that are cleaned in electrostatic precipitator (ESP), semi-dry desulfurization plant (FGD) and fabric filters (FF) before the stack. There are separate flue-gas ducts and flue-gas cleaning systems for each boiler.

The flue gas was studied in two different locations: the flue-gas plume and a reference point inside the stack. Measurements were made at both locations in two different flue-gas cleaning situations: FGD + FF off and, with all cleaning systems, FGD + FF on. The measurement location in the stack was at the height of +35 m above sea level. The flue-gas temperature inside the duct was 78 ± 2 °C in normal operation conditions and 130 ± 13 °C during FGD + FF off. The flue-gas plume concentrations were measured with a helicopter equipped with aerosol instruments. The flying altitude of the helicopter was 150 m above ground level or higher, which corresponds to the lidar (Halo Photonics Streamline Doppler lidar with full-hemispheric scanning capability, Pearson et al., 2009) (Fig. S2) results for plume altitude. It should be noted that only the flue gases from the boiler under investigation were steered to bypass FGD and FF. Thus, in the FGD + FF off situation, the flue-gas plume consisted of both the cleaned flue gas and the flue gas cleaned by ESP. This has to be kept in mind during the analysis of atmospheric measurements.

The measurements were made on 24 March 2014 in two separate 1 h periods (see specific times from Fig. S2, the black rectangles; the first illustrates FGD + FF on and the lat-

ter FGD + FF off). Weather conditions were stable during the study. The wind direction and speed were 216 ± 5.51° (based on lidar data) and 6.5 m s^{-1} in FGD + FF off and 220 ± 6.25° and 4 m s^{-1} in FGD + FF on. The marine boundary layer height was 246–258 m and the planetary boundary layer heights were 360–530 m. However the calculations were made within the marine boundary layer because the flue-gas plume did not rise above it. The background aerosol concentrations for each measured gaseous component were 403 ppm for CO_2 and less than 2–8 ppb for SO_2. The range of ambient temperature was 6.6–6.9 °C, the global radiation was 347–466 W m^{-2} and the visibility was 29 043–36 000 m (see standard deviations from Table S2).

The instrument installations in different locations are shown in Fig. S3. The sampling of flue gas in the stack was performed with a Fine Particle Sampler (FPS; Dekati Ltd., Mikkanen et al., 2001) with total dilution ratio (DR) of 27. Probe and dilution air temperatures were at 200 °C. The sample was analysed using the following instruments: Condensation Particle Counter (CPC3776; TSI Inc., Agarwal and Sem, 1980), Electrical Low Pressure Impactor (ELPI; Dekati Ltd., Keskinen et al., 1992), Scanning Mobility Particle Sizer (SMPS; Wang and Flagan, 1990) 0.6/6 standard L min^{-1} (DMA3071, CPC3775 TSI Inc.) and gas analysers for diluted CO_2 (model VA 3100, Horiba) and NO, NO_2 and NO_x (model APNA 360, Horiba). Measurement data were also received from a normal operation monitoring of the emissions, including raw flue-gas SO_2, NO_x, CO_2 concentrations and dust (SICK RM 230, calibrated based on SFS-EN 13284-1 standard). In contrast to stack sampling, the sample in the flue-gas plume dilutes naturally and can be sampled to equipment without additional dilution of aerosol sample. The sampling inlet position in the helicopter is shown in Fig. S3. Natural dilution causes rapid changes in concentrations, thus high measurement frequency equipment was used in the helicopter. CPC3776 (TSI Inc.) was installed to measure the total particle number concentration, whereas the Engine Exhaust Particle Sizer (EEPS, TSI Inc., Mirme, 1994) measured the particle number size distribution at 1 Hz sampling frequency from 5.6 to 560 nm. Gas concentrations for CO_2/CH_4/H_2O (Cavity spring-down spectrometry Picarro model G1301-m CO_2/CH_4/H_2O flight analyser) and SO_2 (Thermo Scientific Inc. model 43i SO_2 analyser, with 5 s response time) were measured continuously with 1 Hz frequency (see more details in Table S3).

Figure 1 shows the helicopter measurement routes for the FGD + FF on and FGD + FF off situations. The objective of flight routes was to follow the centre line of the flue-gas plume. The helicopter flew both up and down the plume; GPS data were used to separate these two flight situations to calculate the distance and the age of the plume separately.

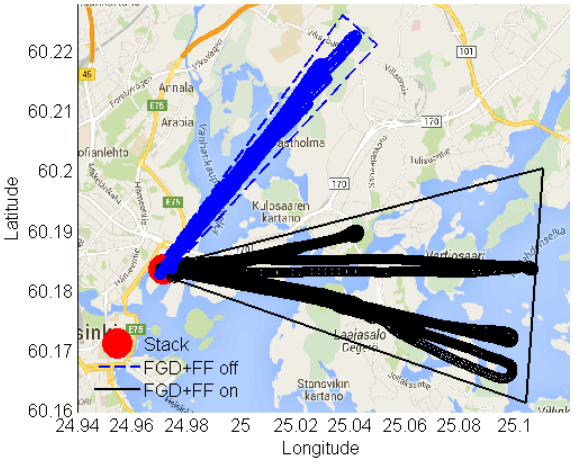

Figure 1. Helicopter flight routes. The wind blew at an angle of 216 ± 5.51° (based on lidar data) and the flight direction was 213 ± 4.14° (based on GPS data for helicopter) in FGD + FF off (blue circles). Corresponding angles for FGD + FF on (black circles) were 220 ± 6.25° (wind direction based on lidar data) and 223 ± 5.66° (flight direction based on GPS data for helicopter). The triangular shapes (black and blue lines) show the helicopter GPS coordinates that have been taken into account in the calculations.

2.1 Model description: Gaussian plume model

The Gaussian plume model is a solution to an advection–diffusion equation that describes the changes in the pollutant concentrations due to advection of wind and turbulent mixing with the surrounding air (Stockie, 2011). Accordingly, the concentration of a pollutant i, C_i, emitted from a point-like source, can be expressed as follows:

$$C_i(x,y,z) = \frac{Q_i}{2\pi U \sigma_y \sigma_z} \exp\left(-\frac{y^2}{\sigma_y^2}\right)\left[\exp\left(-\frac{(z-H)^2}{\sigma_z^2}\right) + \exp\left(-\frac{(z+H)^2}{\sigma_z^2}\right)\right]. \quad (1)$$

Here x, y and z are the spatial coordinates, aligned so that the x axis corresponds to the wind direction and H is the height at which i is emitted (stack height). Also, Q_i is the emission rate of i at the source, U is the mean wind speed and σ_z as well as σ_y are the so-called dispersion coefficients which reflect the spatial extent of the plume as a function of the downwind distance x. The dispersion coefficients were calculated using the parameterization of Klug (1969) and the atmospheric stability class, which is needed to calculate the dispersion coefficients. Atmospheric stability classes were estimated based on the measurements of the wind speed and solar radiative flux at the surface. Moreover, the pollutant concentrations were calculated along the centre line of the plume, the value of U was set to constant and was equal to the average wind speed during the flights. Finally the value of z was set equal to the stack height (150 m).

It is worth noting that the background concentration of i is zero according to Eq. (1): $C_i \to 0$ when $z \to \infty$ or $y \to \pm\infty$. However, the flue gas emitted from the stack was actually cleaner in terms of particle number concentration than the background air when the flue gas was cleaned properly. In order to account for such cases, the following equation was used instead of Eq. (1):

$$\hat{C} = C_\infty + \frac{C_0 - C_\infty}{C_0} \times C_i, \quad (2)$$

where C_∞ is the background concentration of i, and C_0 is its concentration at the source. It can be readily shown that Eq. (2) is a solution to the advection–diffusion equation underlying Eq. (1). Also, it is easily verified that $\hat{C} \to C_\infty$ when $z \to \infty$ or $y \to \pm\infty$. Finally, the value of Q_i in Eq. (1) was chosen so that $\hat{C} \to C_0$ when $z \to H$ and $x,y \to 0$.

An important output of the model is the dilution ratio of the flue-gas plume, DR, which is calculated based on Eq. (3).

$$\mathrm{DR}(t) = \frac{[\mathrm{CO_2}(t)] - [\mathrm{CO_{2,\infty}}]}{[\mathrm{CO_{2,stack}}] - [\mathrm{CO_{2,\infty}}]} \quad (3)$$

In Eq. (3) $[\mathrm{CO_2}(t)]$ and $[\mathrm{CO_{2,\infty}}]$ are the modelled CO_2 concentration at time t and the CO_2 concentration measured in the stack, respectively.

2.1.1 Model description: nucleation rate and particle formation calculations

The particle appearance (driven by nucleation and growth) rates for the particles 2.5 nm in diameter were calculated using the parameterization developed by Lehtinen et al. (2007) presented in Eq. (4). The key input parameters for the model are the nucleation rate (J_{nuc}), the particle growth rate (GR) and the coagulation sink, of which the coagulation sink describes clusters that are removed via coagulational scavenging (CoagS). The parameter J_{nuc} is calculated based on the estimated sulfuric acid concentrations as a function of plume age as detailed below, and the particle growth rates are calculated by assuming growth only via irreversible condensation of sulfuric acid. Also, CoagS is calculated from the condensation sink CS (which is calculated in a fashion described below) using the Eq. (8) in Lehtinen et al. (2007). Also, the initial size of the freshly nucleated clusters was varied, and the value of the shape factor (m in Eq. 6 in Lehtinen et al., 2007) was set equal to -1.6.

$$J_x = J_{\mathrm{nuc}} \times \exp\left(-\gamma \times d_1 \times \frac{\mathrm{CoagS}(d_1)}{\mathrm{CS}}\right) \quad (4)$$

The nucleation rates J_{nuc} in the studied plume were calculated using the parameterization developed by Kulmala et al. (2006), which has also been applied previously to model nucleation in plumes (Stevens et al., 2012; Stevens and Pierce, 2013).

$$J_{\mathrm{nuc}} = A \times [\mathrm{H_2SO_4}] \quad (5)$$

In Eq. (5) $A = 1\times10^{-7}\,\mathrm{s^{-1}}$ or $A = 1\times10^{-6}\,\mathrm{s^{-1}}$ and $[\mathrm{H_2SO_4}]$ ($\mathrm{cm^{-3}}$) is the sulfuric acid concentration. The value of $A = 1\times10^{-7}\,\mathrm{s^{-1}}$ was chosen according to the study by Stevens et al. (2012) and Stevens and Pierce (2013). The initial size of the nucleated particles was assumed to be of 1.5 nm.

Formation of $[\mathrm{H_2SO_4}]$ was calculated assuming that it is produced only via the $\mathrm{OH} + \mathrm{SO_2}$ reaction and the only loss pathway for H_2SO_4 is condensation onto the particle surfaces. When steady-state is assumed, the $[\mathrm{H_2SO_4}]$ can be calculated from Eq. (6).

$$[\mathrm{H_2SO_4}] = k_1 \times \frac{[\mathrm{SO_2}] \times [\mathrm{OH}]}{\mathrm{CS}} \quad (6)$$

In Eq. (6) k_1 is the reaction constant between OH and SO_2 (Table B.2 in Seinfeld and Pandis, 2006). The SO_2 concentrations were taken from the helicopter measurements, and the time development of CS and [OH] in the plume were modelled as follows. First, CS was calculated using the relation shown in Eq. (7).

$$\mathrm{CS} = \frac{\mathrm{CS_{stack}}}{\mathrm{DR}} + \mathrm{CS_\infty} \times \left(1 - \frac{1}{\mathrm{DR}}\right) \quad (7)$$

In Eq. (7) $\mathrm{CS_{stack}}$ is the condensation sink of aerosols measured in the stack, and $\mathrm{CS_\infty}$ is the condensation sink of the background aerosols. The value of the latter parameter was calculated from the size distributions measured at the SMEAR III station (Junninen et al., 2009), which is located around 2 km away from the power plant. Second, [OH] was calculated using the parameterization of Stevens et al. (2012), which has downward shortwave radiative flux at the surface and $[\mathrm{NO}_x]$ as main inputs. The value for the former parameter was taken from the measurements (using the value averaged over the measurement periods), and the NO_x concentrations were calculated from Eq. (8).

$$[\mathrm{NO}_x(t)] = \frac{[\mathrm{NO}_{x,\mathrm{stack}}]}{\mathrm{DR}(t)} \quad (8)$$

In Eq. (8) $[\mathrm{NO}_{x,\mathrm{stack}}]$ is the NO_x concentration measured in the stack. It should be noted here that in the calculations the background concentration of NO_x is assumed to be of minor importance when compared to NO_x emitted by power plants. To support this, the study of Pirjola et al. (2014) indicates that in the harbour area close to the power plant studied, the NO_x concentration level is typically clearly lower than 100 ppb.

3 Results

3.1 Primary emissions of the coal-fired power plant

The SO_2 and particle emissions of the power plant were strongly dependent on the flue-gas cleaning system. This can be seen in Table 1, which shows flue-gas concentrations for CO_2, SO_2, NO_x, O_2, particle number (N_{tot}), dust as well as

Table 1. Flue-gas concentrations of CO_2, SO_2, NO_x, O_2, total particle number (N_{tot}), dust and flue-gas flow rate in the stack. Mean values (and standard deviation) are presented for both flue-gas cleaning conditions (FGD + FF on and FGD + FF off).

	FGD + FF off	FGD + FF on
CO_2 (%)	9.92 ± 2.2	10.3 ± 0.96
SO_2 (ppbv)	$243\,000 \pm 71\,300$	$55\,200 \pm 14\,600$
NO_x (ppmv)	252 ± 74	258 ± 65
O_2 (%)	6.16 ± 0.11	6.11 ± 0.10
N_{tot} (cm^{-3})	$(1.8 \pm 0.2) \times 10^6$	420 ± 640
Dust ($mg\,Nm^{-3}$)	188 ± 82	4 ± 1
Flow ($Nm^3\,h^{-1}$)	$(4.86 \pm 0.20) \times 10^5$	$(4.65 \pm 0.064) \times 10^5$

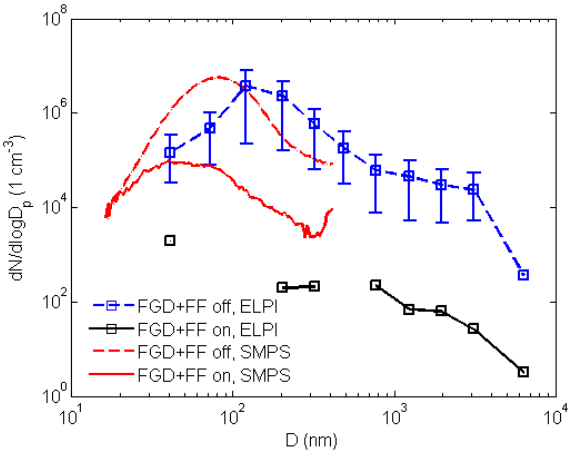

Figure 2. Particle size distributions measured with ELPI and SMPS from the flue gas in the stack. ELPI and SMPS data are shown in operation conditions, FGD + FF on and FGD + FF off. The x axis is aerodynamic diameter for ELPI data and electrical mobility diameter for SMPS data.

flow rate in the duct in both flue-gas cleaning conditions. In the shift from FGD + FF off to FGD + FF on, the SO_2 concentration decreased to nearly a fifth, the concentration of dust decreased by a factor of 50 and the N_{tot} decreased by a factor of 4000. For other parameters the effect of FGD + FF was insignificant.

Figure 2 shows the particle number size distributions of flue gas in the stack in both cleaning conditions. These were measured using an electrical low pressure impactor (ELPI) and a scanning mobility particle sizer (SMPS) in both FGD + FF on/off cases. In the FGD + FF on case, the SMPS measurement is a median value over a few hours of operation due to low particle number concentrations in the stack. Based on the SMPS measurement the particle geometric mean electrical mobility equivalent diameter was 80 nm and the width of particle number size distribution (geometric standard deviation, GSD) was 1.45 for FGD + FF off. In comparison, the geometric mean electrical mobility equivalent diameter was 31 nm for FGD + FF on and the width of particle number size distribution was 2.15. Based on the measurements using the ELPI geometric mean aerodynamic equivalent diameter was 141 nm and GSD was 1.41 for FGD + FF off. The difference in mean diameter measured using the ELPI and the SMPS comes from the difference in size classification principles of these instruments and enables the determination of effective density of measured particles. The effective density calculation is based on the relation between the electrical mobility equivalent diameter and the aerodynamic equivalent diameter of the particle (see Ristimäki et al., 2002). In this study case the difference in equivalent diameter indicates effective density larger than unit density for emitted particles (approximately $3.1\,g\,cm^{-3}$). In comparison, Saarnio et al. (2014) used an effective density of $2.5\,g\,cm^{-3}$ to convert the electrical mobility diameter measured using a SMPS to an aerodynamic diameter. When studying FGD + FF on, the particle concentrations were so low and thus accurate determination of mean particle size was not possible from the particle size distribution measured by the ELPI.

Flue-gas samples from the stack were diluted with hot dilution air before the particle instruments and thus the particle number concentrations (Table 1) and particle size distributions (Fig. 2) are for non-volatile particles. In combustion studies the hot dilution air is typically used to prevent the formation of liquid nucleation particles and to minimize the effects of condensation of semi-volatile compounds on particles. However, to ensure the measured particles were non-volatile and not affected by the dilution method itself, a thermodenuder (Rönkkö et al., 2011) was used periodically after the sampling and dilution. The thermodenuder did not affect the particle number size distribution, which confirms the non-volatile nature of the measured particles. Due to this non-volatility of the particles, the lifetime of the primarily emitted particles in the atmosphere can be longer than that of volatile particles, e.g. nucleation mode particles observed in vehicle exhaust (Lähde et al., 2009).

3.2 Atmospheric measurements

Figure 3 shows the measured flue-gas plume concentrations as a function of plume age. Diffusion losses for the particles in the sampling lines were calculated based on the measurement set-up (see Fig. S4). The data were recorded based on GPS coordinates, which were used to calculate distances from the stack, and the distances were changed to correspond plume age using wind speeds of 6.5 and $4.0\,m\,s^{-1}$ (lidar, Fig. S2). The calculation showed that nearly 70 % of the 2.5 nm particles in diameter was lost in the sampling lines and thus the total concentration shown in Fig. 3 can be higher than shown here. The vertical lines denote the 2 km distance from the stack. Figure 3 shows the dilution timescale of the flue gas in terms of CO_2 and SO_2 in both operation conditions. The same trend in SO_2 and N_{tot} concentrations as observed in Table 1 was measured by instruments installed in

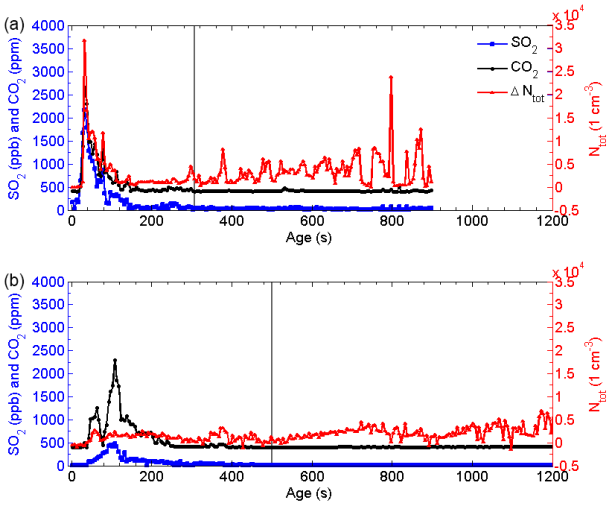

Figure 3. Concentrations of power plant flue-gas components measured by instruments installed in the helicopter as a function of plume age; FGD + FF off in the top panel and FGD + FF on in the bottom panel. SO_2 (ppb, blue line) and CO_2 (ppm, black line) concentrations on the left axes and total particle number concentration ΔN_{tot} (1 cm^{-3}, red line, from CPC) on the right axes. The ΔN_{tot} is calculated using the background value calculated from the upwind side of the stack ($CO_{2,bg}$ was 403 ppm and $SO_{2,bg}$ 2–8 ppb). The grey vertical lines denote 2 km distance from the stack in FGD + FF on/off. The presented results are 5 s median values.

the helicopter; in FGD + FF off the particle and SO_2 concentrations were higher than the FGD + FF on situation. It should be kept in mind that in FGD + FF off only one of the two flue-gas cleaning systems was bypassed.

Plume dilution can be evaluated by the CO_2 concentrations (in Fig. 3a and b), which show that the FGD + FF off case dilutes to approximately background levels in 200 s (0.74 km) and the FGD + FF on case in 300 s (1.5 km). The peak values for CO_2, SO_2 and N_{tot} were 3195 ppm, 2193 ppb, 3.3×10^4 cm^{-3} in the FGD + FF off and 3254 ppm, 585 ppb, 0.4×10^4 cm^{-3} for the FGD + FF on. However, dilution decreases the CO_2, SO_2 and N_{tot} concentrations in the atmosphere to 422 ppm, 52 ppb in FGD + FF off, and 473 ppm, 89 ppb in FGD + FF on. The N_{tot} reached near background concentrations after 200 s and 300 s. The background gaseous concentrations for each measured gaseous component were 403 ppm and 2–8 ppb for CO_2 and SO_2, respectively. The boundary layer mixing started during the FGD + FF on measurements and thus the background values measured from the upwind side flight loops from the stack were averaged and subtracted from both FGD + FF on/off. It can be noted that very near (first 10–50 s) the stack the helicopter was not in the plume. This can be seen from CO_2 and SO_2 concentration values presented in Fig. 3a and b when approaching plume age zero. Thus, the dilution process is discussed below, mainly from the maximum concentrations onward.

An increase in total particle concentration can be seen in Fig. 3 after 400 s aged the flue-gas plume. This tendency can be seen in both flue-gas cleaning situations. Based on Fig. 3a, for the FGD + FF off situation, the background particle concentration was 1430 cm^{-3}, after 200 s the concentration was at the background level and after 400 s it increased significantly, even up to an average level of 5000 cm^{-3}. Based on CO_2 measurements, the dilution of flue gas was practically complete at 200 s. Similarly, in the FGD + FF on situation after 500 s the particle concentration was slightly above background, after which it increased even up to 5000 cm^{-3} after 700 s. Thus, the concentrations in the diluted and aged flue-gas plume were higher than the background and significantly higher than could be expected based on the primary particle concentrations and observed dilution profiles. In general, taking into account the fact that there is no comprehensive measurement of the primary precursor matrix (only $[SO_2]$ is measured), the primary precursor matrix might include low-volatile organics and SO_3, which can increase the probability of new particle formation. Due to the increasing trend in particle concentration, some estimation about formation rates can be calculated. Depending on the plume age, the mean formation rates calculated from the data shown in Fig. 3 depended on the plume age being for FGD + FF off 0–81 cm^{-3} s^{-1} and for FGD + FF on, 0 to 18 cm^{-3} s^{-1} (mean slope of increasing total particle number concentration at 400–482 and 500–692 s).

Particle size distributions, shown in Fig. S5, were calculated from the EEPS data measured from the helicopter in both FGD + FF on/off situations as a 10 s moving median method. The particle size distribution in the FGD + FF off case had a mode around 80 nm, which refers to the solid particle median diameter measured with the SMPS from the flue gas in the stack. The particle size distribution measurement made using the EEPS (Fig. S5) supports the results for total particle number measurement made by the CPC (Fig. 3), i.e. in terms of particles the flue gas dilutes in 0–300 s in FGD + FF off. In addition, the particle size distributions measured by the EEPS indicates a slight increase of nanoparticle concentrations during the dilution and dispersion of the flue gas in the atmosphere. Although EEPS total particle number concentration cannot be compared to total concentration of CPC because Levin et al. (2015) showed that EEPS total particle number concentration is not comparable with a CPC. Further, Fig. S5 shows that the EEPS particle size distribution data are noisy and, based on Awasthi et al. (2013), can show maximum of 67 % error compared to SMPS.

3.3 Model calculations: modelled vs. measured CO_2 concentrations

The validity of the Gaussian plume model was tested against CO_2 measurements from the plume. Median CO_2 concentrations were calculated using the measurement data at a 5 s

Table 2. Comparison between modelled CO_2 concentration and measured CO_2 concentration, and comparison between SO_2 measured from the atmosphere and Gaussian-model-diluted SO_2. Mean relative error (MRE) and correlation coefficients (R^2) were calculated between measured and modelled concentrations.

		CO_2		SO_2	
case	stab. class	MRE (%)	R^2	MRE (%)	R^2
FGD + FF off	c	5	0.97	131	0.95
	d	25	0.97	322	0.96
FGD + FF on	b	29	0.87	291	0.84
	c	40	0.87	413	0.85

interval separately for the FGD + FF on/off cases and the locations of the peak CO_2 concentration (t_{max}, $[CO_{2,max}]$) were identified from the resulting time series. The value C_0 was chosen for Eq. (2) so that the modelled CO_2 concentration, $\hat{C}_{CO_2}$, was around $[CO_{2,max}]$ when $t = t_{max}$. The choice of C_0 was made in this manner rather than initializing the model to use the stack concentrations due to the following two reasons. First, the Gaussian plume model does not yield reliable results close to the source, i.e. within a few tens of metres (Arya, 1995). Second, the comparison of the results near (first 10–50 s) the source is problematic because the helicopter was not located at the plume centre line during the initial stages of the measurements.

Comparison of the measured and modelled CO_2 concentrations is shown in Fig. 4 and in Table 2. The chosen stability classes were b and c for FGD + FF on and c and d for FGD + FF off, corresponding to the stability conditions ranging from unstable to neutral (Pasquill, 1961). As can be seen, the model reproduces the observed trends rather well, in particular for FGD + FF off, while the model tends to slightly overestimate the observed concentrations for FGD + FF on. The modelled and measured concentrations were within one standard deviation in general. Mean relative error (MRE) and correlation coefficients (R^2) were calculated between the measured and modelled concentrations for CO_2. In order to further investigate the performance of the model, a comparison was made between measured SO_2 and Gaussian-model-diluted SO_2 concentrations, shown in Fig. S6 and Table 2. The results showed that the model consistently overestimates the SO_2 concentration in the plume, typically by a factor between 3 and 4, compared to the measured values. This difference could be partly explained by the oxidation of SO_2 because it is not taken into account by the model. However, this discrepancy between MREs and R^2 does not affect the model performance as the measured SO_2 concentrations, instead of being modelled, were used in the plume model simulations.

3.4 Model calculations: nucleation and new particle formation

Modelled and measured CO_2 concentrations showed that the model reproduced the observed dispersion of the plume relatively accurately. Thus the model was applied to calculate $[NO_x]$, [OH] and $[H_2SO_4]$, which were needed to investigate the possibility of new particle formation in the plume. These results are summarized in Fig. 5. It is seen that sulfuric acid concentrations exponentially increase during the initial stages of the simulation and then reach constant concentration around 1×10^6 and 1×10^7 cm^{-3}, a range which is also comparable to the atmospheric observations of $[H_2SO_4]$ (Mikkonen et al., 2011) formation. Mikkonen et al. (2011) reported that H_2SO_4 concentrations varied between 1.86×10^5–2.94×10^6 molec cm^{-3} and Sarnela et al. (2015) reported $[H_2SO_4]$ concentrations 4.4×10^6–11.5×10^6 molec cm^{-3} for Finnish industrial and non-industrial area. More H_2SO_4 is formed in the FGD + FF off case because of higher primary SO_2 emission compared to the FGD + FF on case.

Initially, OH concentrations are lowered by large concentrations of NO_x which subsequently decrease during plume ageing. NO_x reduction leads to increases in [OH] and $[H_2SO_4]$. While the [OH] increased consistently during

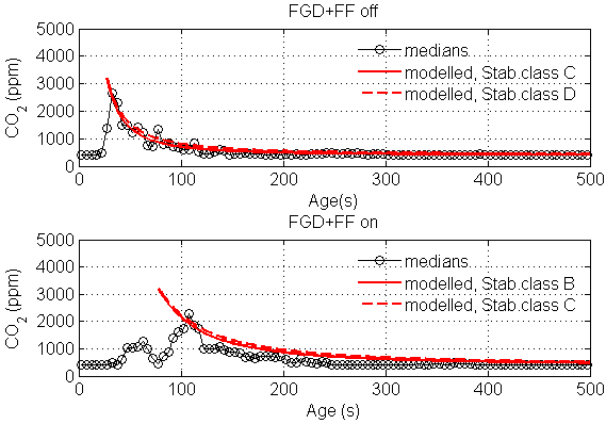

Figure 4. Comparison of measured and modelled CO_2 concentrations. Median of measured values are shown with black (circle) symbols along with the standard deviations. Dashed and dotted red lines correspond to model results for stability classes b and c (top panel) and c and d (bottom panel), respectively. The correlation coefficients between the model and the measurements are shown in Table 2.

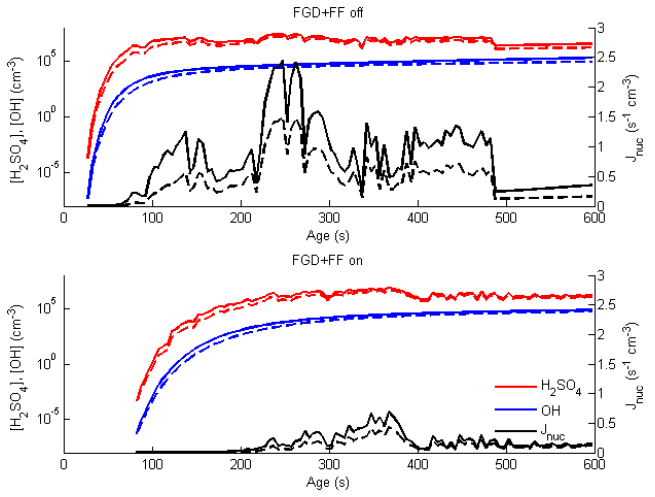

Figure 5. Time development of $[H_2SO_4]$ (red lines), nucleation rate (black lines), [OH] (blue lines) (cm^{-3}). Dashed and dotted red lines correspond to model results for stability classes c and d (top panel) and b and c (bottom panel), respectively.

the simulations, $[SO_2]$ decreased because of dilution. Due to these opposed trends, the production term for the sulfuric acid in Eq. (6), did not change greatly during the later stages of the simulations. Moreover, the condensation sink (CS) diluted rapidly to its background value, which was around $1 \times 10^{-2}\,s^{-1}$. These facts explain why the modelled sulfuric acid concentrations, calculated with Eq. (6), did not change notably after the initial rapid increase.

The modelled nucleation rate J_{nuc} is directly proportional to the sulfuric acid concentration and hence the trends in $[H_2SO_4]$ are directly reflected in J_{nuc} (Fig. 5). Furthermore, in our measurements the particles were detected at the lowest CPC detection limit which was 2.5 nm, $J_{2.5}$. According to the scheme applied here (see Eqs. 4 and 5), the fraction of freshly nucleated particles that survive into detectable sizes depends mainly on their growth rate (GR) and condensation sink (CS). The average given by the model GRs were 0.34 or 0.19 $nm\,h^{-1}$ in the FGD + FF off case, and 0.07 or 0.04 $nm\,h^{-1}$ in the FGD + FF on case for the two stability class scenarios. These values are clearly smaller than atmospheric GR observations in urban areas (e.g. Stoltzenburg et al., 2005). As a lower GR leads to a lower surviving fraction, we conclude that the modelling results do not explain the observed particle formation in the flue-gas plume.

A series of additional calculations were performed in order to investigate the sensitivity of the results to the values of the key input parameters. First, J_{nuc} is proportional to the constant A, the exact value of which is not accurately known, and this uncertainly translates directly into the calculated nucleation rates. A sensitivity analysis was made for the nucleation model in order to evaluate the sensitivity of nucleation rates to the value of A (shown in Table 3). In these calculations, a value of 1×10^{-6} was chosen for A, which is an order of magnitude higher than in base case simulations. The choice of the value was based on the study of Sihto et al. (2006) who investigated NPF (new particle formation) events occurring in boreal forest. As can be seen, an increased value of A alone is not sufficient to explain observed new particle formation. A second source of uncertainty is the sulfuric acid concentration, which was calculated using a rather simple scheme (see Sect. 2.1.1). Increases in $[H_2SO_4]$ leads to both increased J_{nuc} and GR and ultimately to larger $J_{2.5}$. Results displayed in Table 3 show that $J_{2.5}$ is more consistent with observations when $[H_2SO_4]$ is increased 5 or 10-fold and when A is set equal to 1×10^{-6} like in Sihto et al. (2006). Therefore, underestimation of $[H_2SO_4]$ may explain the discrepancy between the observations and base case model results. This might be caused by underestimation of [OH] or overestimation of CS. Regarding the modelled OH concentrations, it can be noted that they are relatively low, reaching values of around $1 \times 10^5\,cm^{-3}$ by the end of the flights. In comparison, concentrations of around $1 \times 10^6\,cm^{-3}$ have been reported during the daytime around noon in various atmospheric environments (Hofzumahaus et al., 2009; Petäjä et al., 2009), 0.26×10^6 molec cm^{-3} in Mace Head (Berresheim et al., 2002), and 1×10^6–2×10^7 molec cm^{-3} in Atlanta (Kuang et al., 2008). Relatively low modelled OH concentrations can be explained by high NO_x concentrations which were calculated to decrease consistently from several tens of ppm down to around 200 ppb during the flights (not illustrated here). Such high concentrations of NO_x are consistent with low [OH] (see Fig. 1 in Lonsdale et al., 2012). It could thus be speculated that the model underestimates $[H_2SO_4]$ and consequently the rate of new particle formation due to overestimation of $[NO_x]$. Moreover, it should be noted that neither SO_3 nor low-volatile organic vapours that might have been present in the measured flue gas were not accounted for in the modelling study. Previous studies suggest that these exhaust compounds may also increase the formation rate of nucleation particles (Pirjola et al., 2015; Ehn et al., 2012; Arnold et al., 2012), which may explain the discrepancy between measurements and model calculations. Regarding the estimation of the value of CS, it should be noted that its values were taken from the field site measurements located nearby rather than from in situ measurements. Therefore it can be speculated that actual CS values were lower than those used as input to the model, which causes additional uncertainties.

3.5 Discussion

Each power plant (over 50 MW) in the EU has emission limits for SO_2, NO_2 and particle mass concentrations. For the studied power plant the limits are 600 mg Nm^{-3} (210 ppm), 600 mg Nm^{-3} (290 ppm) and 50 mg Nm^{-3}. A comparison of the results in Table 1 with these emission limits shows that the emissions were clearly below these limits when the power plant operation was normal (FGD + FF on). It was observed that these low emissions can be achieved through properly

Table 3. Sensitivity analysis made for number of particles formed with diameters above 2.5 nm during the flight ($1\,cm^{-3}\,s^{-1}$) in the atmosphere with different values of A and $[H_2SO_4]$. The $[H_2SO_4]$ is calculated based on the measurement results and scaled up to test faster nucleation rates for both FGD + FF on and FGD + FF off cases and stability classes (sc).

$A = 1 \times 10^{-7}\,s^{-1}$							
	sc	$1 \times [H_2SO_4]$	$1.25 \times [H_2SO_4]$	$1.5 \times [H_2SO_4]$	$2 \times [H_2SO_4]$	$5 \times [H_2SO_4]$	$10 \times [H_2SO_4]$
FGD + FF off	b	1.00×10^{-4}	5.36×10^{-4}	1.73×10^{-3}	8.29×10^{-3}	0.289	1.74
	c	0	0	0	4.32×10^{-4}	4.78×10^{-2}	0.44
FGD + FF on	c	0	0	0	0	4.27×10^{-4}	1.85×10^{-2}
	d	0	0	0	0	0	1.73×10^{-3}
$A = 1 \times 10^{-6}\,s^{-1}$							
	sc	$1 \times [H_2SO_4]$	$1.25 \times [H_2SO_4]$	$1.5 \times [H_2SO_4]$	$2 \times [H_2SO_4]$	$5 \times [H_2SO_4]$	$10 \times [H_2SO_4]$
FGD + FF off	b	1.00×10^{-3}	5.36×10^{-3}	1.73×10^{-2}	8.29×10^{-2}	2.89	17.4
	c	0	0	4.47×10^{-4}	4.32×10^{-3}	0.48	4.43
FGD + FF on	c	0	0	0	0	4.27×10^{-3}	0.19
	d	0	0	0	0	0	0.017

working flue-gas cleaning systems. In addition to primary emissions, flue-gas cleaning systems also seemingly affect the compounds, which can act as precursors for new particles, e.g. SO_2 tends to oxidize in the atmosphere to form SO_3 and further forms H_2SO_4, which can nucleate or condensate to particle phase. This study clearly shows the importance of flue-gas cleaning technologies and underlines the proper usage of the technologies when the atmospheric pollution is discussed in terms of coal combustion. For example, according to Huang et al. (2014) in Xi'an and Beijing 37 % of the sulfate in atmospheric particles is emitted from coal burning.

In this study the power plant plume diluted to background levels in 2 km (200–400 s), which is faster than in other in-flight measurements (Stevens et al., 2012; Junkermann et al., 2011). This difference may be because the dilution of plume and other processes are affected by source strength, background concentrations and meteorology (Stevens et al., 2012). We observed that while SO_2 and CO_2 were already diluted to background levels, the effect of the source to aerosol concentration was still clearly distinguishable after 2 km. In our study, we collected high time-resolution data close to the power plant stack, which enabled us to model the plume dilution on a detailed scale. From this, we were able to observe that while SO_2 and CO_2 were already diluted to background levels at a distance of 2 km – in agreement with the dilution modelling – the effect of the source on the aerosol number concentration was distinguished at distances > 2 km. We attribute this to nucleation taking place in the ageing plume.

According to the modelling results from Stevens et al. (2012), atmospheric new particle formation via nucleation of sulfuric acid begins in the flue-gas plume at 1 km distance from the coal-fired power plant, whereas the sulfuric acid formation begins right after emission. Our study therefore supports this previous modelling work by showing that nucleation may take place in the aged plume and is most effective after 400 s, corresponding to a distance of approximately 2 km from the emission source in the atmosphere.

In light of the new results authors would like to distinguish the primary particle emission from the newly formed particle emission because those particles have different effects on the atmosphere and different formation mechanisms. By comparing primary particle emission with newly formed particle emission, the effects of different particles in the atmosphere could be taken into account more precisely in aerosol models or air quality assessments.

For instance, rough estimates for particle number emission factors can be calculated by comparing the measured particle number concentration with the simultaneously measured CO_2 concentration of the flue-gas plume (see e.g. Saari et al., 2016). By utilizing this method for particles existing in the flue-gas plume between the ages of 25–55 s, the emission factor with respect to CO_2 was $2.0 \times 10^{10}\,(g\,CO_2)^{-1}$, as well as from ages over 400 s $8 \times 10^{10}\,(g\,CO_2)^{-1}$ in the FGD + FF off case. Similarly, in the FGD + FF on case, the emission factors were $4 \times 10^{9}\,(g\,CO_2)^{-1}$ (for aerosol dispersed 55–85 s in the atmosphere) and $3.74 \times 10^{10}\,(g\,CO_2)^{-1}$ (for aerosol dispersed more than 500 s in the atmosphere). In comparison, the primary emissions were $1.75 \times 10^{10}\,(g\,CO_2)^{-1}$ for FGD + FF off and $8.0 \times 10^{6}\,(g\,CO_2)^{-1}$ for FGD + FF on. Thus, new particle formation can increase the real atmospheric particle number emissions even by several orders of magnitude. It should be noted that particle formation depends strongly on the plume age $[SO_2]$ and primary particle concentrations, and it is possible that there are some low-volatile organics or SO_3 present in the plume, affecting the nucleation.

Our observations show that the number of secondary particles formed in the flue-gas plume can be several orders of

magnitude higher than the primary particles directly emitted from the flue-gas duct. The formation can already be observed at a distance of ca. 2 km from the stack; this distance is significantly lower than the grid size used in many atmospheric models, which demonstrates the need for subgrid parameterizations for power-plant-originating secondary particles. Such a parameterization does already exist (Stevens and Pierce, 2013), but it does not account for different types of sulfur removal technologies such as semi-dry desulfurization and wet desulfurization. Determining the effect of different removal technologies on power plant secondary aerosol production would increase the accuracy of particle-loading predictions for regional air quality and global models.

4 Conclusions

Emissions of a coal-fired power plant into the atmosphere were studied comprehensively for the first time, by combining direct atmospheric measurements, measurements conducted in the power plant stack, and modelling studies for atmospheric processes of flue-gas plume. The stack measurements were made to estimate the effectiveness of flue-gas cleaning technologies, such as filtering and desulfurization. It was shown that the flue-gas cleaning technologies had a great effect on the SO_2 and total particle number concentrations in the primary emission. SO_2 concentration was reduced to fifth of FGD + FF off compared to FGD + FF on and the total non-volatile particle number concentration was reduced by several orders of magnitude. A similar trend in primary emission reduction was detected in the atmospheric measurements. In addition, the reduction in primary emissions directly affects the concentrations of gaseous precursors (SO_2) for secondary particle formation in the atmosphere.

It was observed that the flue gas dilutes to background concentrations in 200–300 s. This dilution timescale is faster than reported in previous studies. However, the concentration profiles also showed an increase in particle number concentration in an aged flue gas, dilution and dispersion processes. To validate the dilution timescale, a Gaussian model was used to calculate the dilution in the atmosphere, taking into account the primary emission and weather conditions. The Gaussian model confirms the dilution timescale, and the dilution ratio could be used to calculate the theoretical maximum values for different components in the flue-gas plume. Weather conditions and theoretical maximum value for [NO_x] were used to calculate the [OH] formation rate and further [H_2SO_4] formation rate. These were calculated because the measurement results showed an increase in particle number concentrations in the flue-gas plume during the dilution process. The modelling results for [H_2SO_4] formation rate support the hypothesis of sulfuric acid formation, but the sulfuric acid formation itself does not totally explain the increase in the total particle number concentration, therefore, e.g. low-volatile organics may exist on the flue-gas plume. The sensitivity analysis of the [H_2SO_4] formation showed that the atmospheric parameterization is not enough to explain the processes in the flue-gas plume.

Comparison between the primary particles and newly formed particles show that in the flue-gas plume of coal-fired power plant, the concentration of newly formed atmospheric particles can be several orders of magnitude higher than the primary particles from the flue-gas duct; therefore they should be considered when discussing emissions of power production. Including the effect of varying flue-gas cleaning technologies in parameterizations of power-plant-originating secondary particles is a necessary step in understanding their importance.

The Supplement related to this article is available online at doi:10.5194/acp-16-7485-2016-supplement.

Acknowledgements. The study was conducted in the MMEA WP 4.5.2. of Cleen Ltd., funded by Tekes (the Finnish Funding Agency for Technology and Innovation). Authors would like to acknowledge Anna Kuusala and Joni Heikkilä for programming Matlab, Aleksi Malinen for measurement help. Fanni Mylläri acknowledges TUT Graduate School, KAUTE-foundation, TES-foundation for financial support. Eija Asmi and Ewan O'Connor acknowledge the support of the Academy of Finland Centre of Excellence program (project number 272041). Ville Vakkari acknowledges the financial support of the Nessling foundation (grant 201500326) and the Academy of Finland Finnish Center of Excellence program (grant 1118615). Fanni Mylläri and Topi Rönkkö acknowledge the financial support from the Academy of Finland ELTRAN (grant 293437).

Edited by: F. Khosrawi

References

Agarwal, J. K. and Sem, G. J.: Continuous Flow, Single-particle Counting Condensation Nucleus Counter, J. Aerosol Sci., 11, 343–357, 1980.

Arnold, F., Pirjola, L., Rönkkö, T., Reichl, U., Schlager, H., Lähde, T., Heikkilä, J., and Keskinen, J.: First online measurements of sulfuric acid gas in modern heavy-duty diesel engine exhaust: Implications for nanoparticle formation, Environ. Sci. Technol., 46, 11227–11234, 2012.

Arya, S. P.: Modeling and parameterization of near-source diffusion in weak winds, J. Appl. Meteorol., 34, 1112–1122, 1995.

Awasthi, A., Wu, B.-S., Liu, C.-N., Chen, C.-W., Uang, S.-N., and Tsai, C.-J.: The effect of nanoparticle morphology on the measurement accuracy of mobility particle sizers, MAPAN-J. Metrol. Soc. I., 28, 205–215, 2013.

Berresheim, H., Elste, T., Tremmel, H. G., Allen, A. G., Hansson, H.-C., Rosman, K., Dal Maso, M., Mäkelä, J. M., and Kulmala,

M.: Gas-Aerosol relationships of H_2SO_4, MSA, and OH: Observations in the coastal marine boundary layer at Mace Head, Ireland, J. Geophys. Res., 107, 8100, doi:10.1029/2000JD000229, 2002.

Brock, C. A., Washenfelder, R. A., Trainer, M., Ryerson, T. B., Wilson, J. C., Reeves, J. M., Huey, L. G., Holloway, J. S., Parrish, D. D., Hübler, G., and Fehsenfeld, F. C.: Particle growth in the plumes of coal-fired power plants, J. Geophys. Res., 107, 4155, doi:10.1029/2001JD001062, 2002.

Buonanno, G., Anastasi, P., DiIorio, F., and Viola, A.: Ultrafine particle apportionment and exposure assessment in respect of linear and point sources, Atmospheric Pollution Research, 1, 36–43, 2012.

Charlson, R. J., Schwartz, S. E., Hales, J. M., Cess, R. D., Coakley Jr., J. A., Hansen, J. E., and Hofmann, D. J.: Climate Forcing by Anthropogenic Aerosols, Science New Series, 255, 423–430, 1992.

Ehn, M., Kleist, E., Junninen, H., Petäjä, T., Lönn, G., Schobesberger, S., Dal Maso, M., Trimborn, A., Kulmala, M., Worsnop, D. R., Wahner, A., Wildt, J., and Mentel, Th. F.: Gas phase formation of extremely oxidized pinene reaction products in chamber and ambient air, Atmos. Chem. Phys., 12, 5113–5127, doi:10.5194/acp-12-5113-2012, 2012.

EU: The EU Emissions Trading System (EU ETS), available at: http://ec.europa.eu/clima/policies/ets/index_en.htm, last access 15 December 2014.

Frey, A. K., Saarnio, K., Lamberg, H., Mylläri, F., Karjalainen, P., Teinilä, K., Carbone, S., Tissari, J., Niemelä, V., Häyrinen, A., Rautiainen, J., Kytömäki, J., Artaxo, P., Virkkula, A., Pirjola, L., Rönkkö, T., Keskinen, J., Jokiniemi, J., and Hillamo, R.: Optical and Chemical Characterization if Aerosols Emitted from Coal, Heavy and Light Fuel Oil, and Small-Scale Wood Combustion, Environ. Sci. Technol., 48, 827–836, 2014.

Helble, J. J.: A model for the air emissions of trace metallic elements from coal combustors equipped with electrostatic precipitators, Fuel Process. Technol., 63, 125–147, 2000.

Hofzumahaus, A., Rohrer, F., Lu, K., Bohn, B., Brauers, T., Chang, C.-C., Fuchs, H., Holland, F., Kita, K., and Kondo, Y.: Amplified trace gas removal in the troposphere, Science, 324, 1702–1704, 2009.

Huang, R.-J., Zhang, Y., Bozzetti, C., Ho, K.-F., Cao, J.-J., Han, Y., Daellenbach, K. R., Slowik, J. G., Platt, S. M., Ganonaco, F., Zotter, P., Wolf, R., Pieber, S. M., Bruns, E. A., Grippa, M., Ciarelli, G., Piazzalunga, A., Schwikowsko, M., Abbaszade, G., Schnelle-Kreis, J., Zimmerman, R., An, Z., Szidat, S., Baltenspergerm, U., El Haddad, I., and Prévôt, A. S. H.: High secondary aerosol contribution to particulate pollution during haze event in China, Nature, 514, 218–222, 2014.

Junkermann, W., Hagemann, R., and Vogel, B.: Nucleation in the Karlsruhe plume during the COPS/TRACKS-Lagrange experiment, Q. J. Roy. Meteor. Soc., 137, 267–274, 2011.

Junninen, H., Lauri, A., Keronen, P., Aalto, P., Hiltunen, V., Hari, P., and Kulmala, M.: Smart-SMEAR: on-line data exploration and visualization tool for SMEAR stations, Boreal. Environ. Res., 14, 447–457, 2009.

Keskinen, J., Pietarinen, K., and Lehtimäki, M.: Electrical Low Pressure Impactor, J. Aerosol Sci., 23, 353–360, 1992.

Klug, W.: A method for determining diffusion conditions from synoptic observations, Staub-Reinhalt. Luft, 29, 14–20, 1969.

Kuang, C., McMurry, P. H., McCormick, A. V., and Eisele, F. L.: Dependence of nucleation rates on sulphuric acid vapor concentration in diverse atmospheric locations, J. Geophys. Res., 113, D10209, doi:10.1029/2007JD009253, 2008.

Kulmala, M., Lehtinen, K. E. J., and Laaksonen, A.: Cluster activation theory as an explanation of the linear dependence between formation rate of 3 nm particles and sulphuric acid concentration, Atmos. Chem. Phys., 6, 787–793, doi:10.5194/acp-6-787-2006, 2006.

Lähde, T., Rönkkö, T., Virtanen, A., Schuck, T. J., Pirjola, L., Hämeri, K., Kulmala, M., Arnold, F., Rothe, D., and Keskinen, J.: Heavy duty diesel engine exhaust aerosol particle and ion measurements, Environ. Sci. Technol., 43, 163–168, 2009.

Lee, S. W., Herage, T., Dureau, R., and Young, B.: Measurement of $PM_{2.5}$ and ultra-fine particulate emissions from coal-fired utility boilers, Fuel, 108, 60–66, 2013.

Lehtinen, K. E. J., Dal Maso, M., Kulmala, M., and Kerminen, V.-M.: Estimating nucleation rates from apparent particle formation rates and vice versa: Revised formulation of the Kerminen-Kulmala equation, J. Aerosol Sci., 38, 988–994, 2007.

Lelieveld, J. and Heintzenberg, J.: Sulfate Cooling Effect on Climate Through In-Cloud Oxidation of Anthropogenic SO_2, Science New Series, 258, 117–120, 1992.

Levin, M., Gudmundsson, A., Pagels, J. H., Fiers, M., Mølhave, K., Löndahl, J., Jensen, K. A., and Koponen, I. K.: Limitations in the Use of Unipolar charging for Electrical Mobility Sizing Instruments: A Study of the Fast Mobility Particle Sizer, Aerosol Sci. Tech., 49, 556–565, 2015.

Lonsdale, C. R., Stevens, R. G., Brock, C. A., Makar, P. A., Knipping, E. M., and Pierce, J. R.: The effect of coal-fired power-plant SO_2 and NO_x control technologies on aerosol nucleation in the source plumes, Atmos. Chem. Phys., 12, 11519–11531, doi:10.5194/acp-12-11519-2012, 2012.

Marris, H., Deboudt, K., Augustin, P., Flament, P., Blond, F., Fiani, E., Fourmentin, M., and Delbarre, H.: Fast changes in chemical composition and size distribution of fine particles during the near-field transport of industrial plumes, Sci. Total Environ., 427–428, 126–138, 2012.

Mikkanen, P., Moisio, M., Keskinen, J., Ristimäki, J., and Marjamäki, M.: Sampling method for particle measurements of vehicle exhaust, SAE 2001 World Congress, 5–8 March 2001, Detroit, Michigan, USA, SAE Technical Paper Series, 2001-01-0219, 2001.

Mikkonen, S., Romakkaniemi, S., Smith, J. N., Korhonen, H., Petäjä, T., Plass-Duelmer, C., Boy, M., McMurry, P. H., Lehtinen, K. E. J., Joutsensaari, J., Hamed, A., Mauldin III, R. L., Birmili, W., Spindler, G., Arnold, F., Kulmala, M., and Laaksonen, A.: A statistical proxy for sulphuric acid concentration, Atmos. Chem. Phys., 11, 11319–11334, doi:10.5194/acp-11-11319-2011, 2011.

Mirme, A.: Electric aerosol spectrometry, PhD Thesis, Tartu University, Tartu, Estonia, 1994.

Pasquill, F.: The estimation of the dispersion of windborne material, The Meteorological Magazine, 90 , 33–49, 1961.

Pearson, G., Davies, F., and Collier, C.: An analysis of the Performance of the UFAM Pulsed Doppler Lidar for observing the Boundary Layer, J. Atmos. Ocean. Tech., 26, 240–250, doi:10.1175/2008JTECHA1128.1, 2009.

Petäjä, T., Mauldin, III, R. L., Kosciuch, E., McGrath, J., Nieminen, T., Paasonen, P., Boy, M., Adamov, A., Kotiaho, T., and

Kulmala, M.: Sulfuric acid and OH concentrations in a boreal forest site, Atmos. Chem. Phys., 9, 7435–7448, doi:10.5194/acp-9-7435-2009, 2009.

Pirjola, L., Pajunoja, A., Walden, J., Jalkanen, J.-P., Rönkkö, T., Kousa, A., and Koskentalo, T.: Mobile measurements of ship emissions in two harbour areas in Finland, Atmos. Meas. Tech., 7, 149–161, doi:10.5194/amt-7-149-2014, 2014.

Pirjola, L., Karl, M., Rönkkö, T., and Arnold, F.: Model studies of volatile diesel exhaust particle formation: are organic vapours involved in nucleation and growth?, Atmos. Chem. Phys., 15, 10435–10452, doi:10.5194/acp-15-10435-2015, 2015.

Ristimäki, J., Virtanen, A., Marjamäki, M., Rostedt, A., and Keskinen, J.: On-line measurement of size distribution and effective density of submicron aerosol particles, J. Aerosol Sci., 33, 1541–1557, 2002.

Rönkkö, T., Arffman, A., Karjalainen, P., Lähde, T., Heikkilä, J., Pirjola, L., Rothe, D., and Keskinen, J.: Diesel exhaust nanoparticle volatility studies by a new thermodenuder with low solid nanoparticle losses, 15th ETH Conference on Combustion Generated Nanoparticles, Zürich ETH Zentrum, 26–29 June 2011, Zurich, Switzerland, 2011.

Saari, S., Karjalainen, P., Ntziachristos, L., Pirjola, L., Matilainen, P., Keskinen, J., and Rönkkö, T.: Exhaust particle and NO_x emission performance of an SCR heavy duty truck operating in real-world conditions, Atmos. Environ., 126, 136–144, doi:10.1016/j.atmosenv.2015.11.047, 2016.

Saarnio, K., Frey, A., Niemi, J. V., Timonen, H., Rönkkö, T., Karjalainen, P., Vestenius, M., Teinilä, K., Pirjola, L., Niemelä, V., Keskinen, J., Häyrinen, A., and Hillamo, R.: Chemical composition and size of particles in emissions of coal-fired power plant with flue gas desulphurization, J. Aerosol Sci., 73, 14–26, 2014.

Sarnela, N., Jokinen, T., Nieminen, T., Lehtipalo, K., Junninen, H., Kangasluoma, J., Hakala, J., Taipale, R., Schobesberger, S., Sipilä, M., Larnimaa, K., Westerholm, H., Heijari, J., Kerminen, V.-M., Petäjä, T., and Kulmala, M.: Sulphuric acid and aerosol particle production in the vicinity of an oil refinery, Atmos. Environ., 119, 156–166, 2015.

Seinfeld, J. H. and Pandis, S. N.: Atmospheric chemistry and physics: from air pollution to climate change, second edition, John Wiley & Sons Inc., New York, USA, 2006.

Sihto, S.-L., Kulmala, M., Kerminen, V.-M., Dal Maso, M., Petäjä, T., Riipinen, I., Korhonen, H., Arnold, F., Janson, R., Boy, M., Laaksonen, A., and Lehtinen, K. E. J.: Atmospheric sulphuric acid and aerosol formation: implications from atmospheric measurements for nucleation and early growth mechanisms, Atmos. Chem. Phys., 6, 4079–4091, doi:10.5194/acp-6-4079-2006, 2006.

Srivastava, R. K. and Jozewicz, W.: Flue Gas Desulfurization: The State of the Art, J. Air Waste Manage., 51, 1676–1688, 2001.

Stevens, R. G. and Pierce, J. R.: A parameterization of subgrid particle formation in sulfur-rich plumes for global- and regional-scale models, Atmos. Chem. Phys., 13, 12117–12133, doi:10.5194/acp-13-12117-2013, 2013.

Stevens, R. G., Pierce, J. R., Brock, C. A., Reed, M. K., Crawford, J. H., Holloway, J. S., Ryerson, T. B., Huey, L. G., and Nowak, J. B.: Nucleation and growth of sulfate aerosol in coal-fired power plant plumes: sensitivity to background aerosol and meteorology, Atmos. Chem. Phys., 12, 189–206, doi:10.5194/acp-12-189-2012, 2012.

Stockie, J. M.: The Mathematics of Atmospheric Dispersion Modeling, SIAM Review, 53, 349–372, 2011.

Stolzenburg, M. R., McMurry, P. H., Sakurai, H., Smith, J. N., Mauldin III, R. L., Eisele, F. L., and Clement, C. F.: Growth rates of freshly nucleated atmospheric particles in Atlanta, J. Geophys. Res., 110, D22S05, doi:10.1029/2005JD005935, 2005.

Wang, S. C. and Flagan, R. C.: Scanning Electrical Mobility Spectrometer, Aerosol Sci. Tech., 13, 230–240, 1990.

Yi, H., Hao, J., Duan, L., Tang, X., Ning, P., and Li, X.: Fine particle and trace element emissions from an anthracite coal-fired power equipped with bag-house in China, Fuel, 2008, 87, 2050–2057, 2008.